Comprehensive study of the formation of stable colloids of Cu Al layered double hydroxide assisted by double hydrophilic block copolymers

G. Layrac, Simon Harrisson, Mathias Destarac, Corine Gerardin, D. Tichit

Comprehensive study of the formation of stable colloids of Cu-Al Layered Double Hydroxide assisted by Double Hydrophilic Block Copolymers

G. Layrac[1,†], S. Harrisson[2], M. Destarac[2], C. Gérardin[1*], D. Tichit[1*]

[1]ICGM, Univ. Montpellier, CNRS UMR 5253, ENSCM, Montpellier, France

[3]IMRCP, UMR 5623 CNRS-UPS Toulouse, France

Corresponding authors.

E-mail address: didier.tichit@enscm.fr; corine.gerardin@enscm.fr

[†]Present address: ICPEES, CNRS UMR 7515, ECPM-Université de Strasbourg, France

Abstract

The formation of stable aqueous colloidal suspensions of Cu-Al layered double hydroxide (LDH) assisted by double-hydrophilic block copolymers was investigated. It was of utmost importance since the direct preparation LDH colloids of controlled size is still a major challenge ; moreover, regarding the Cu-Al system, the mechanism of formation of the LDH phase is not well understood yet. Cu-Al LDH nanoparticles were obtained by complexing Cu^{2+} and Al^{3+} cation mixture ($Cu^{2+}/Al^{3+} = 2$) with an asymmetric poly(acrylamide)-*b*-poly(acrylic acid) block copolymer, followed by metal cation hydroxylation. The mechanism of formation of the Cu-Al LDH was studied and compared to that of Mg-Al LDH. ICP-MS analysis of the hybrid polyion complex (HPIC) micelles obtained at increasing complexation ratio, i. e. the ratio of the molar concentration of complexing acrylate group of DHBC to M^{2+} and Al^{3+} cations ($R = AA/(M^{2+} + Al^{3+})$), showed higher selectivity of DHBC toward Al^{3+} and, among M^{2+} cations, for Cu^{2+} than for Mg^{2+}. Hydroxylation of the HPIC micelles led to macroscopic precipitates at R values below flocculation thresholds, ie. R1 = 0.43 for DHBC/Cu-Al and 0.13 for and DHBC/Mg-Al suspensions, while stable suspensions were formed above R1. The hydrodynamic diameter (D_h)

of the colloids determined by DLS decreased from 160 to 50 nm and from 350 to 50 nm in the DHBC/Cu-Al and DHBC/Mg-Al colloids, respectively, when R increased from R1 to 1. XRD and TEM analyses of the dried colloidal suspensions (R > R1) revealed the presence of Cu-Al LDH and Mg-Al LDH phases and elemental analyses confirmed that M(II)/Al = 2. Particle sizes were lower in Cu-Al LDH than in Mg-Al LDH. Titration curves corresponding to progressive hydroxylation of DHBC/Cu(or Mg)-Al solutions at fixed complexation ratio R allowed establishing that formation of Cu-Al and Mg-Al LDH obeyed to a similar sequential mechanism in two steps but involving different aluminum hydroxide precursors according to the different pH values of precipitation. Cu-Al LDH was obtained by combination of aluminum poly(hydr)oxide species with dissolved copper-based species at pH ~ 5.5, while Mg-Al LDH resulted from combination of $Al(OH)_3$ and dissolved Mg^{2+} at pH ~ 8.

Key words

Layered double hydroxide; Double hydrophilic block copolymers; Hybrid polyion complex micelles; Magnesium; Copper; Aluminum.

1. Introduction

The preparation of stable aqueous suspensions of layered double hydroxide (LDH) nanoparticles or LDH nanosheets offer large perspectives in several application fields including catalysis, biomedicine …(Wang et al., 2005; Xu et al., 2006; Li et al., 2011; Wang and O'Hare, 2012; Zhang et al., 2016; Mao et al., 2017). An efficient and fully colloidal route for nanoparticle synthesis was previously developed by some of us for the direct preparation of aqueous colloidal stable suspensions of metal (hydr)oxides of Al^{3+}, La^{3+}, Cu^{2+}, Ni^{2+} or Zn^{2+}, of ZnS, and, recently, of Mg-Al LDH (Gérardin et al., 2003; Bouyer et al., 2003, 2006; Tarasov et al., 2013; Layrac et al., 2014). This method relies on the use of asymmetric double hydrophilic block copolymers (DHBC), such as poly(acrylamide)-*b*-poly(acrylic acid) (PAm-

b-PAA) polymers, which act as both, growth control and stabilizing agents. In the case of Mg-Al LDH, the synthesis process consists in mixing Mg^{2+} and Al^{3+} cations with the DHBC, yielding hybrid polyion complex (HPIC) micelles which contained only Al^{3+}, while Mg^{2+} ions remained free in solution. Then progressive hydroxylation of DHBC/Al^{3+} micelles leads to DHBC/aluminum hydroxide colloids, which integrate increasing amounts of Mg^{2+} ions, leading ultimately to precipitation of Mg-Al LDH phase in the core of the HPIC micelles acting as confined nanoreactors. The ratio of the molar concentration of complexing acrylate groups to Mg^{2+} and Al^{3+} cations ($R = AA/(Mg^{2+} + Al^{3+})$) allowed controlling the extent of growth of the LDH particles and the stability of the colloids. The mechanism of formation of the LDH phase taking place in the micellar core, above described (Layrac et al., 2014), was in agreement with the classical one described in the literature when trivalent metal hydroxides more soluble than divalent metal hydroxides were involved (Boclair and Braterman, 1999; Seron and Delorme, 2008). On the contrary, it was reported that when the divalent and trivalent metal hydroxides exhibit close solubility, LDH phases were directly precipitated (Boclair and Braterman, 1998; Boclair et al., 1999; Rhada et al., 2003). Such behavior was observed when Cr^{3+} on one hand and Zn^{2+}, Co^{2+} or Ni^{2+} on the other hand were involved as metal cationic species (Boclair and Braterman, 1998; Boclair et al., 1999). Direct formation of LDH phase was also claimed when using mixtures of Al^{3+} or Cr^{3+} and Cu^{2+} cations. This is unexpected due to the very different solubility of the trivalent metal hydroxides and of $Cu(OH)_2$. Besides no clear evidence of the formation of the Cu-Al LDH phase was provided (Depège at al., 1996; Boclair and Braterman, 1998). These previous studies revealed on one hand that a given cation mixture leads to a specific pH of coprecipitation of the LDH phase, depending on the relative solubility of the divalent and trivalent metal hydroxides. On the other hand, LDH formation can follow different pathways during precipitation depending on the nature of the cations. Cu-containing LDH are known for their great potential as precursors of supported copper-based catalysts; their

preparation as stable nanoparticles is then highly desirable. However, due to the remarkable efficiency of Cu^{2+} among divalent cations to form HPIC micelles (Layrac et al., 2015), the formation of Cu-Al LDH colloids assisted by complexing DHBC represents a major challenge. Moreover, the mechanism of formation of Cu-Al LDH during titration of a mixed Cu^{2+}- Al^{3+} solution was not well established yet. Indeed $Al(OH)_3$ and $Cu(OH)_2$ simple hydroxides precipitate at close values of pH (pH ~5) (Figure S1), then there was some doubt about the sequential or direct coprecipitation mechanism of formation of Cu-Al LDH. This question is particularly relevant when confinement in the HPIC micelle core is involved. Preparation of Cu-Al LDH following different protocols was previously described in the literature, however with scarce investigations on the formation mechanisms. Bukhtiyarova (2019) reported that pure Cu-Al LDH was obtained when coprecipitation was performed at pH values in the range 7 – 8 depending on the nature of the precursor anionic salts. Park et al. (1990) obtained pure Cu-Al LDH from copper(II) ammine solution and aluminum sulfate. Boclair and Braterman (1998) pointed out that Cu-Al LDH forms directly from the sulfate salts. Besides, another peculiar aspect of the Cu-containing LDH was underlined since the pioneer review of Cavani et al. (1991) who reported that they can form only when another divalent cation, e. g. Zn^{2+}, Co^{2+} or Mg^{2+}, was present. This behavior was assigned to distorsion of the octahedral coordination structure due to the cooperative Jahn -Teller effect. Several studies of synthesis of very useful multicationic Cu-containing LDH as catalyst precursors have indeed confirmed that pure crystallographic LDH phases were obtained in wide ranges of $\Sigma M^{2+}/M^{3+}$ atomic ratios with M^{2+} = Cu^{2+}, Ni^{2+}, Co^{2+}, Zn^{2+}, Mg^{2+} and M^{3+} = Al^{3+} and/or Fe^{3+}, and at varying co-precipitation pHs. Marchi et al., 2003; Trujillano et al., 2005; Raciulete et al., 2014; Li et al., 2015; Zhang et al., 2017; Lucarelli et al., 2018; Said et al., 2018; Lu et al., 2019) That confirms the versatility of copper to form LDH phases in systems combining several divalent and/or trivalent cations and suggests that the Jahn-Teller effect in Cu-Al LDH was cleverly overpassed by separating Cu

cations in the brucite-like layers of multicationic LDH. Then, in addition to insights into the mechanism of formation, a relevant objective of the present work was to obtain pure Cu-Al LDH phase through the direct colloidal synthesis route from HPIC micelles. A main drawback for the formation of Cu-Al LDH through the HPIC micelle route, could result from the higher complexing ability of DHBC for Cu^{2+} than for the other transition metal ions, i. e. Ni^{2+}, Co^{2+}, Mn^{2+}, Cu^{2+}, Zn^{2+} (Layrac et al., 2015) in agreement with its peculiar position in the series of Irving-Williams referring to the stability constants of formation of high-spin complexes (Irving and Williams, 1953). Therefore, due to the high DHBC-Cu^{2+} affinity, competitive complexation will be far less favorable to Al^{3+} than in the case of Mg^{2+}. That feature will also participate to induce a mechanism of formation of the Cu-Al LDH different from that of the Mg-Al LDH in the presence of DHBC.

In summary, there are three main reasons which concur to render the formation of Cu-Al LDH from HPIC micelles a challenging task: i) the close precipitation pHs of the simple $Al(OH)_3$ and $Cu(OH)_2$ hydroxides, ii) the formation of pure Cu-containing LDH phase more easily achieved in the presence of other divalent or trivalent cations, and iii) the high selectivity of PAA complexing block for Cu^{2+}.

The present paper focuses on the mechanism of formation of the Cu-Al LDH in the presence and in the absence of asymmetric PAm_{10000}-*b*-PAA_{1500} DHBC. A comparison with the Mg-Al system in the same synthesis conditions was also achieved. First, the composition of the micelles obtained upon complexation of the Cu-Al and Mg-Al mixtures at increasing complexation ratio was studied by ICP-MS. Then the colloids resulting from the metal hydroxylation in the micelles were characterized by light scattering and the LDH phase was identified by XRD. Finally, the progressive hydroxylation of the HPIC micelles at a fixed metal complexation ratio was carefully followed. These studies led us to establish a mechanism of formation of the Cu-Al LDH -based hybrid colloids.

2. Experimental section

2. 1. Materials

The DHBC polymer used was a poly(acrylamide)-*b*-poly(acrylic acid) (PAm-*b*-PAA) in which the PAA metal-binding block is smaller than the PAm neutral block. The chemical formula of the PAm-*b*-PAA DHBC is presented below:

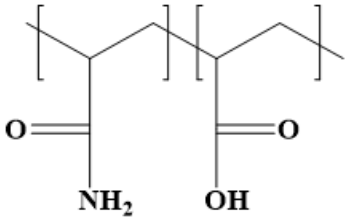

The number-averaged molecular weights (Mn) of the PAA and PAm blocks are 1500 g mol^{-1} and 10000 g mol^{-1}, respectively, they are indicated close to each block name, as follows: PAm_{10000}-*b*-PAA_{1500}. This DHBC polymer was prepared according to a well-established RAFT/MADIX polymerization of acrylic acid (AA) in aqueous solution using a macroxanthate PAmXA1 (Layrac et al., 2015). $MgCl_2$. 6 H_2O, $CuCl_2$. 2 H_2O and $AlCl_3$. 6 H_2O (Sigma Aldrich) were used as sources of metal cations. Deionized water (Purelab, Elga, France) was always used for the preparation of the solutions.

The synthesis of colloidal suspensions of hybrid LDH nanoparticles proceeds in two steps, i. e. micellization and mineralization steps.

2. 2. Micelle formation

An aqueous solution of $CuCl_2$. 6 H_2O (or $MgCl_2$. 6 H_2O), $AlCl_3$. 6 H_2O (atomic ratio M(II)/Al = 2) was prepared with concentrations [Cu^{2+} (or Mg^{2+})] = 10^{-1} mol/L and [Al^{3+}] = 5.10^{-2} mol/L. Separately, an aqueous solution of PAm_{10000}-*b*-PAA_{1500} at a concentration of 6.4 . 10^{-4} mol/L in

acrylate function was prepared. Its pH was adjusted at 5.5, which corresponds to a degree of dissociation of the acrylic acid groups of about 50%. The two solutions were then mixed, the amount of PAm_{10000}-*b*-PAA_{1500} added to the cation solution depended on the complexation ratio R, which was defined as the molar ratio of acrylate groups (AA) per total amount of cations (R = AA/(M(II)+Al)); R was varied from 0 to 1. To maintain Cu(or Mg) and Al concentrations in the micelle suspensions constant at $[M^{2+}] = 10^{-2}$ mol/L and $[Al^{3+}] = 5.10^{-3}$ mol/L whatever the R values, deionized water was added in order to obtain a final volume of 5 ml. The solutions were stirred for 10 min before the mineralization step.

2. 3. Mineralization by coprecipitation at constant pH of Cu(or Mg)-Al cation solutions with varying amounts of DHBC copolymer

LDH formation was induced by co-hydroxylation of Cu^{2+}(or Mg^{2+}) and Al^{3+} at a constant pH of 8.5 and 10 for Cu^{2+} and Mg^{2+}, respectively, upon addition of increasing amounts of a NaOH solution (0.2 mol/L) under air atmosphere. 5 ml aqueous solution containing 0.5 ml solution of cations (Cu(or Mg)/Al = 2; $[M^{2+}] = 10^{-1}$ mol/L and $[Al^{3+}] = 5.10^{-2}$ mol/L) and the DHBC polymer in varying amounts (R varied from 0 to 1) was added at a feeding rate of 0.4 ml/min in 5 ml of deionized water, whose pH was maintained at 8.5 (Cu^{2+}) or 10 (Mg^{2+}) by addition of NaOH (0.2 mol/L). The final volume of suspension was of 10 ml. The colloidal suspensions were then stored at ambient temperature in closed flasks. Final concentrations of $[M^{2+}] = 5 . 10^{-3}$ mol/L and $[Al^{3+}] = 2.5 . 10^{-3}$ mol/L were thus obtained in the DHBC/LDH suspensions.

2. 4. Mineralization by progressive hydroxylation of a Cu(or Mg)-Al cation solution in the absence and in the presence of DHBC copolymer (R = 0.8)

Without DHBC: 5 ml aqueous solution containing 0.5 ml cation solution (Cu(or Mg)/Al =2; $[Cu^{2+}$(or $Mg^{2+})] = 10^{-1}$ mol/L and $[Al^{3+}] = 5.10^{-2}$ mol/L) was titrated with NaOH (0.4 mol/L).

The hydroxylation degree h is defined as the molar ratio of OH ions per cation (h = OH/(Cu(or Mg) + Al)). h was varied from 0 to 2.6.

With DHBC: 5 ml aqueous solution containing 0.5 ml cation solution (Cu(or Mg)/Al = 2; $[M^{2+}]$ = 10^{-2} mol/L and $[Al^{3+}]$ = 5.10^{-2} mol/L) and the amount of DHBC polymer to obtain R = 0.8 was titrated with NaOH (0.4 mol/L). h was varied from 0 to 2.6.

2. 5. Characterization methods

The dynamic light scattering (DLS) measurements were performed at 25 °C using a Malvern Autosizer 4800 spectrogoniometer, with a 50 mW laser source operating at 532 nm. The scattering measurements were done at a scattering angle of 90°. The measured normalized time correlation function was analyzed by using the CONTIN algorithm. The values of the hydrodynamic diameter were calculated from the decay times using Stokes-Einstein equation: $Dh = k_BT/3\pi\eta D$ where k_B is the Boltzmann constant, T the absolute temperature, η the solvent viscosity, and D the diffusion coefficient. The Dh values are intensity-averaged hydrodynamic diameters.

Powder X-Ray diffraction (XRD) patterns were recorded using a Bruker D8 Advance Diffractometer and the monochromatic Cu-Kα1 radiation (λ_α = 0.154184 nm, 40 kV and 50 mA). They were recorded with a 0.02° (2θ) step over the 2–70° 2θ angular range with 0.2 s counting time per step. The acquisition of XRD pattern was performed on powders obtained by evaporation of the colloidal suspensions on glass slides at 40 °C during 2 hours.

Elemental analysis of the elements in the dried colloidal suspensions precipitated in dioxane was carried out by inductively coupled plasma-mass spectra ICP-MS Agilent 7700, for which the samples were dissolved in 66% HNO_3 solution.

Transmission electron microscopy (TEM) analysis was performed on the suspensions diluted 10 times. A drop was placed on a carbon-copper grid, and after a few minutes of evaporation

in air at ambient temperature, the remaining solution was sucked with a filter paper to obtain a few particles on the grid. The sample was then characterized using a Jeol 1200 EXII microscope operated at 80 kV. The particle size distributions were determined using the Measure It software.

3. **Results and discussion**

The nature of the intermediate micelles during the formation of stable aqueous suspensions of PAm_{10000}-*b*-PAA_{1500} DHBC/Cu-Al LDH colloids was studied, followed by an investigation of the hydroxylation step leading to the precipitation of the Cu-Al LDH phase. It was compared to the mechanism of formation of the PAm_{10000}-*b*-PAA_{1500} DHBC/Mg-Al LDH colloids in the same experimental conditions in order to highlight the specificity induced by Cu^{2+}. A previous study dealing with the complexation by PAm-*b*-PAA of a series of divalent transition metal cations, i. e. Ni^{2+}, Co^{2+}, Mn^{2+}, Cu^{2+} and Zn^{2+}, revealed the higher selectivity for Cu^{2+} (Layrac et al., 2015). Consequently, the competition between cations for complexation by PAm-*b*-PAA DHBC might be more favorable to Cu^{2+} than Mg^{2+} in a M^{2+} - Al^{3+} (M^{2+} = Mg^{2+} or Cu^{2+}) mixture of ions. To check this hypothesis, the formation of HPIC micelles was investigated with mixtures of Cu^{2+}-Al^{3+} and of Mg^{2+}-Al^{3+} cations (M^{2+}/Al^{3+} = 2) and asymmetric PAm_{10000}-*b*-PAA_{1500} DHBC at increasing complexation ratio R ($0.33 \leq R \leq 1$). The micelles were precipitated in a bad solvent of the PAm block (dioxane in this case) and analyzed by ICP-MS. Characterization by DLS and identification by XRD of the LDH phase were then performed on the colloidal suspensions ($0 \leq R \leq 1$) after hydroxylation by NaOH. Finally, the hydroxylation step was investigated in details by performing progressive hydroxylation of the DHBC/Cu-Al and DHBC/Mg-Al mixtures prepared at R = 0.8.

3. 1. Formation of hybrid micelles in the DHBC/Cu-Al system and comparison with the DHBC/Mg-Al system

Micelle suspensions were prepared by mixing the DHBC solution (pH = 5.5) with the mixed metal cation solutions. Speciation of the DHBC/Cu-Al and DHBC/Mg-Al mixtures previously precipitated in dioxane known as a bad solvent for PAm blocks was first performed (Sanson et al., 2005; Layrac et al., 2014). The metal cation yields in the obtained precipitates, as determined by ICP-MS, were reported in Table 1. In the two systems, the Al^{3+} yields increase from ~ 8% at R = 0.33 to 46.4% at R = 1 for DHBC/Mg-Al and from 10% at R = 0.33 to 52.5% at R = 1 for DHBC/Cu-Al; these similar values were clearly higher than the corresponding yields in divalent cations. Moreover, a great difference was noted between the Mg^{2+} and Cu^{2+} yields. The Mg^{2+} yield did not exceed 1% while the Cu^{2+} yield reached 3.5% at R = 1. Accordingly, the M(II)/Al atomic ratios lay in the range from 0.02 to 0.04 and from 0.005 to 0.13 with Mg-Al and Cu-Al mixtures, respectively, for R values between 0.33 and 1 (Table 1). The M(II)/Al ratios, though increasing with R values, remained by far lower than the nominal value of 2. Therefore, the obtained micelles can be considered as Mg-free DHBC/Al^{3+} micelles in the case of the Mg^{2+}-Al^{3+}mixture as previously reported with the less asymmetric PAA_{3000}-*b*-PAm_{10000} DHBC polymer (Layrac et al., 2014). In the case of Cu^{2+}-Al^{3+} mixture, complexation of Al^{3+} ions took place preferentially, though a small amount of Cu^{2+} ions were also present in the micelles above R = 0.5. These results confirmed the higher selectivity of PAm_{10000}-*b*-PAA_{1500} DHBC, on one hand toward trivalent cations and on the other hand, for Cu^{2+} rather than for Mg^{2+}.

Table 1: Yields of M^{2+} and Al^{3+} and M^{2+}/Al^{3+} atomic ratios in the PAm_{10000}-*b*-PAA_{1500}/M(II)-Al micellar systems as a function of R value, as determined by ICP-MS.

R[a]	DHBC/Mg-Al		DHBC/Cu-Al	
	Mg/Al	Al^{3+}		Cu/Al

	Al^{3+}	Mg^{2+}		Yield (%)	Cu^{2+}	
	Yield (%)	Yield (%)			Yield (%)	
0.33	8.00	0.03	0.017	10.0	0.23	0.005
0.53	21.3	0.38	0.027	29.5	0.08	0.054
0.66	28.1	0.45	0.032	36.1	1.59	0.052
0.8	34.4	0.72	0.037	43.2	2.32	0.107
1	46.4	1.00	0.041	52.5	3.46	0.131

[a]R= AA/(M(II)+Al)

3. 2. Hydroxylated DHBC/Cu-Al colloids obtained at increasing copolymer amount and comparison with the Mg-Al system

The DHBC/Cu-Al mixture (Cu^{2+}/Al^{3+} ratio of 2) was titrated by increasing the hydroxylation ratio h ($h = OH^-/(Cu^{2+} + Al^{3+})$) from 0 to 3.5 using a NaOH solution. The titration curve and the corresponding dpH/dh derived curve allowed choosing the pH value for coprecipitation of the DHBC/Cu-Al colloidal suspensions that ensured formation of the LDH phase (Figure S1). For comparison, the titration curves of Cu^{2+} and Al^{3+} ions alone, with NaOH, were also reported. In the case of Cu^{2+} alone, an abrupt pH increase from 5 to 13 was observed corresponding to an equivalent point (h_{eq}) value of ca. 1.5 accounting for precipitation of paratacamite $Cu_2(OH)_3Cl$ phase in agreement with the use of Cu and Al chloride precursor salts. In the case of titration of Al^{3+}, the plateau observed at pH = 4.6 followed by the pH increase with h_{eq} value of 3 at pH = 6 well corresponded to the precipitation of $Al(OH)_3$ in the speciation diagram (Baes, 1976). Regarding the Cu-Al mixture (without DHBC), the titration curve presented a plateau at pH 4 – 5 and an abrupt pH increase between pH 6 and 11. The h_{eq} value of 2 at pH = 8.5 corresponded to coprecipitation of the Cu-Al LDH phase. Thereafter, we chose

the pH value of 8.5 to coprecipitate the Cu^{2+} and Al^{3+} cations in the DHBC/Cu-Al mixtures. DHBC/Mg-Al mixtures studied for sake of comparison were coprecipitated at pH = 10 as previously established (Layrac et al., 2014).

Therefore, investigations were performed on DHBC/Cu-Al and DHBC/Mg-Al micelle suspensions hydroxylated at pH = 8.5 and 10, respectively, obtained at R values increasing from 0 to 1. The same general evolution of the macroscopic aspect of both types of suspensions was observed (Figure 1). In the absence of DHBC (R = 0), blue/green and white precipitates were observed for Cu-Al and Mg-Al metal cation mixtures, respectively. They corresponded to Cu-Al and Mg-Al LDH phases as confirmed by XRD patterns recorded on the dried powders exhibiting in both cases at 11.54° and 23.02° (2Θ) reflections assigned to (003) and (006) basal reflections, respectively (Figure 2). In the presence of DHBC, macroscopic precipitates were still observed at low R values when there was not enough acrylate entities able to complex the cations, which then precipitated upon NaOH addition. Above a minimal R value corresponding to the flocculation threshold and designated as R1, precipitates were not observed; stable turbid and opalescent suspensions were formed. Noteworthy, very different values of R1 of 0.43 for DHBC/Cu-Al and 0.13 for DHBC/Mg-Al suspensions were obtained. As R was increased further above R1, both suspensions became less turbid and were transparent at R = 1.

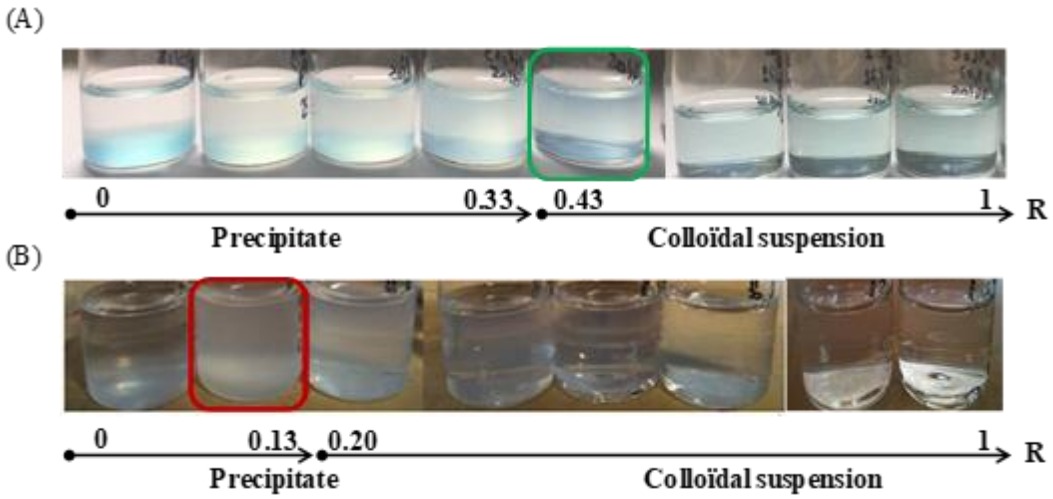

Figure 1: Macroscopic aspect of (A) DHBC/Cu-Al and (B) DHBC/Mg-Al solutions obtained at R values increasing from 0 to 1. (Samples corresponding to the R1 values of the flocculation thresholds are indicated in green (A), and in red (B)).

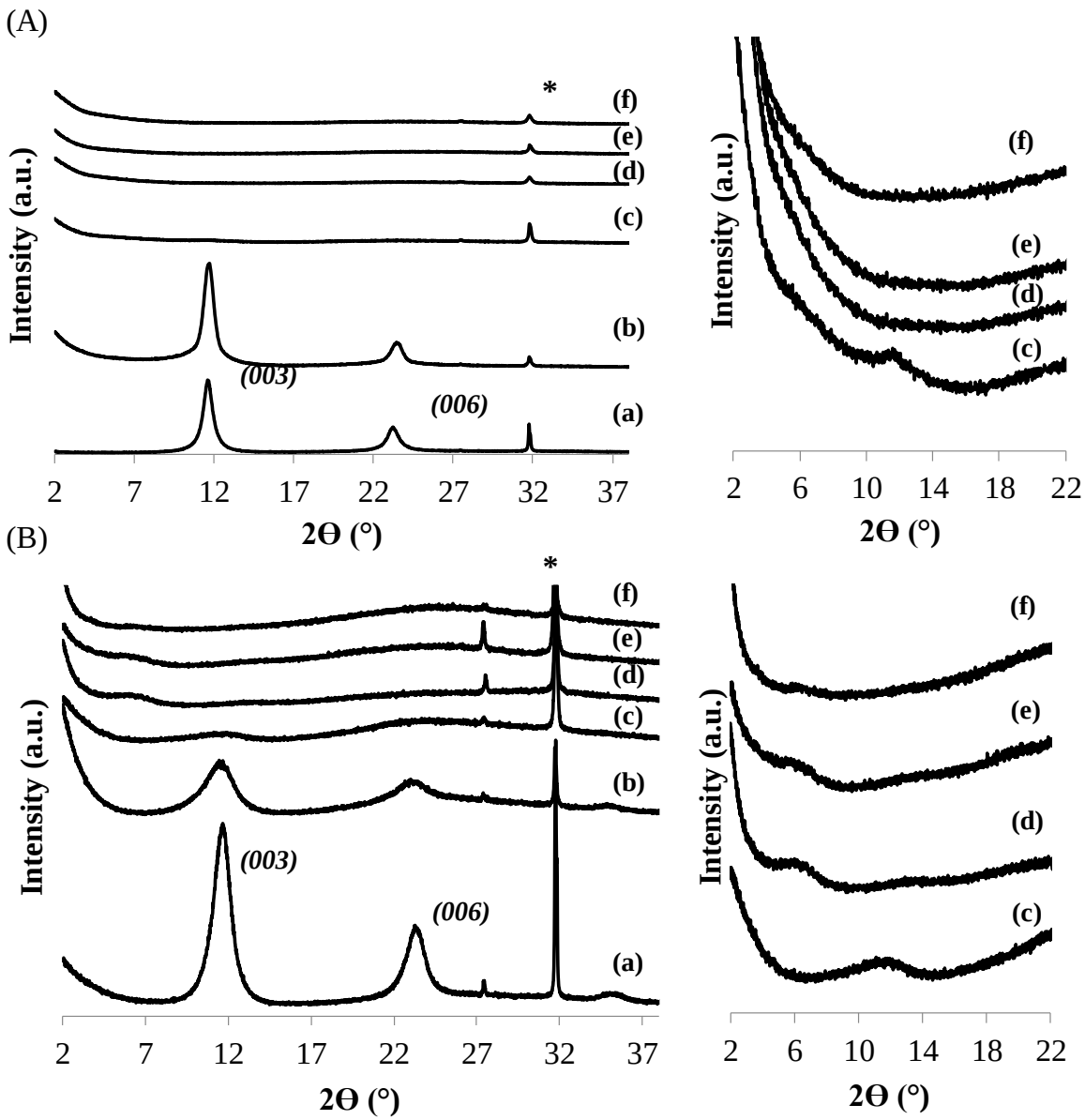

Figure 2: Powder XRD patterns of (A) Cu-Al LDH at R = 0 (a); macroscopic precipitate at R = 0.13 (b), 0.33 (c); dried Cu-Al LDH colloids at R = 0.43 (d), 0.53 (e) and 0.66 (f); (B) Mg-Al LDH at R = 0 (a); macroscopic precipitate at R = 0.05 (b); dried Mg-Al LDH colloids at R = 0.13 (c), 0.33 (d), 0.66 (e) and 0.80 (f) (*NaCl).

DLS analyses were performed on the aqueous supernatants recovered below R1 and on the stable colloidal suspensions obtained above R1. The variations of the scattered intensities of

the hydroxylated DHBC/Cu-Al and DHBC/Mg-Al colloids as a function of R were reported on Figure 3. The same general evolution was observed for the two types of colloids. The intensity first increased sharply up to the flocculation threshold, i. e. R1 = 0.43 and 0.13 for Cu-Al and Mg-Al systems, respectively. The intensity increase is due to the presence of increasing amounts of stable colloidal species in the suspensions. After a maximum, the scattered intensity decreased smoothly then became stable and similar for the two systems above R = 0.8. The hydrodynamic diameter (D_h) of the colloids followed the same evolution. It decreased from 160 to 50 nm when R increased from 0.43 to 1 in the DHBC/Cu-Al colloids and from 350 to 50 nm when R increased from 0.13 to 1 in the DHBC/Mg-Al ones. It must be noted that the Dh values of the DHBC Mg-Al colloids were larger at the flocculation threshold than those of the DHBC/Cu-Al colloids. As no precipitate was formed in this range of R values, all LDH particles were contained in the core of the colloids. The decrease of D_h as a function of the complexation degree accounted for the formation of a higher amount of smaller particles whose external surface was stabilized by the copolymers.

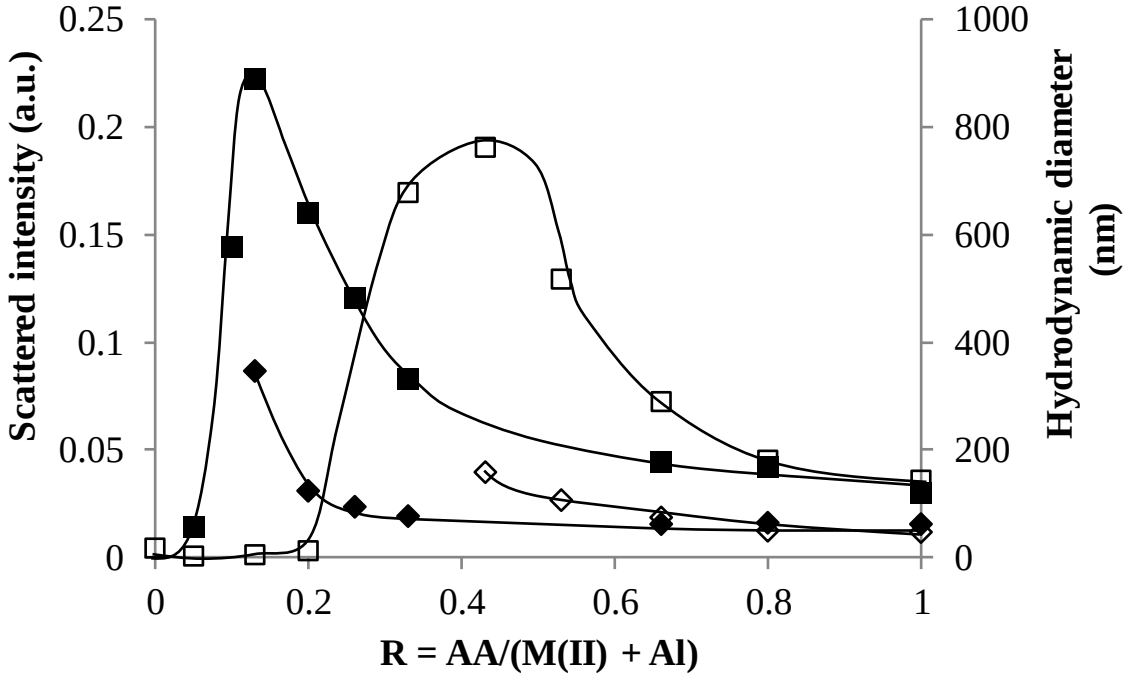

Figure 3: Scattered intensity (■, □) and hydrodynamic diameter (♦, ◊) as a function of the complexation ratio R of colloidal PAm_{10000}-*b*-PAA_{1500}/Cu-Al LDH (empty symbol) and PAm_{10000}-*b*-PAA_{1500}/Mg-Al LDH (full symbol) particles.

The presence of the LDH phase in the colloids was checked by recording the powder XRD patterns of the films recovered after evaporation of several drops of suspensions on a glass slide. In the case of the Cu-Al system the XRD pattern of the macroscopic precipitate obtained at R = 0.13, i. e. below R1, was, as expected, similar to that of the reference sample (R = 0) and corresponded to Cu-Al/CO_3^{2-} LDH phase (Figure 2A). The d003-value of 0.766 nm and d006-value of 0.386 nm could indistinctly correspond to the intercalation of Cl^- or CO_3^{2-} in the LDH structure. However, CO_3^{2-} provided by CO_2 dissolved in the synthesis solution was more likely intercalated due both to its higher selectivity and higher concentration ($[CO_3^{2-}]$ = ~ 45 . 10^{-3} mol/L) than Cl^- present in lower amount in the very diluted cation salt solutions ($[Cl^-]$ = 17.5 . 10^{-3} mol/L). The reflection at 31.7° (2Θ) corresponded to NaCl formed during coprecipitation

of the LDH phase by reaction of NaOH with the precursor chloride salts. NaCl was not eliminated because no washing step was included in our experimental protocol. For the colloidal suspensions, only the most intense (003) reflection at 11.54° (2Θ) corresponding to d003-value of 0.77 nm and the intercalation of CO_3^{2-} was observed at R = 0.33, which then vanished when R increased to 0.53 and 0.66. These features revealed the presence of stable colloidal suspensions of Cu-Al LDH particles. In the case of the Mg-Al system, the XRD pattern of the macroscopic precipitate obtained at R = 0.05, i. e. below the R1 value (R1 = 0.13), was similar to the reference sample (R = 0) (Figure 2B). The XRD pattern of the evaporated colloid at the flocculation threshold R1 = 0.13 exhibited (003) and (006) reflections of weak intensity corresponding to the intercalation of CO_3^{2-}. At all R > R1 values only a very weak (003) reflection shifted to d003-value of 1.26 nm was detected. This basal reflection corresponded to the intercalation of the negatively charged PAA block of the DHBC which indeed acted as charge compensating anion of the LDH as R increases (Layrac et al., 2014). The wider and less intense (00l) diffraction peaks observed for the Cu-Al LDH in comparison to the Mg-Al LDH above R1 suggested particle sizes of lower dimension in the c direction with a lower amount of stacked layers.

TEM analysis of the dried colloids has also been performed in order to characterize the morphology of the LDH phases. For the Cu-Al system (Figure S2) the macroscopic precipitate obtained at R = 0 (without DHBC) showed aggregated anisotropic LDH particles with average size higher than 80 nm in the (a, b) direction. The images of the DHBC/Cu-Al LDH colloidal suspension evaporated on the TEM grid obtained at R = 0.33, i. e. below the flocculation threshold (R = 0.43), also showed a high density of muddled and anisotropic particles of low thickness. The average size in the (a, b) direction was in the range from 40 to 50 nm with only 2 to 3 stacked nanosheets. This probably resulted from inhibition of growth in the c direction due to adsorption of DHBC on the (a, b) planes. The density and muddle as well as the average

size of the particles greatly decreased for R values above R1. Average particle sizes of 40 and 30 nm were indeed found at R = 0.53 and 0.66, respectively. Measurement of the distance between two successive sheets observed on LDH particles obtained at R = 0.66, allowed to determine an interlayer space of ~1.3 nm in agreement with intercalation of the negatively charged polyacrylate chains. For the Mg-Al system (Figure S3), TEM image of the Mg-Al LDH macroscopic precipitate obtained at R = 0.05, well below the flocculation threshold (R1 = 0.13), showed a high density of particles in the range of 50 – 100 nm. For DHBC/Mg-Al LDH colloids obtained above R1, and evaporated on the grid, the tendency is toward a decrease of the particles aggregation as R increased, though they are still muddled. Their size was in the range from 5 to 45 nm at R = 0.20. In both Cu-Al and Mg-Al systems an increase of the degree of complexation allowed to reduce the aggregation and the mean size of the LDH particles formed in the core of the colloids. However, these evolutions were observed in slight different extents in the Cu-Al LDH and Mg-Al LDH, the former leading to lower aggregation degree and mean size.

M(II)/Al atomic ratios in the PAm_{10000}-*b*-PAA_{1500}/Cu(or Mg)-Al colloids recovered by precipitation in dioxane before and after hydroxylation were determined as a function of R increasing from R1 to 1 by ICP-MS. As reported above in the study of the micelle formation, the atomic ratios obtained before hydroxylation were very low in both series but slightly higher for Cu/Al than for Mg/Al. They were by far lower than the nominal values of 2 and their increase with R revealed that increasing the amounts of complexing functions favored divalent metal ion complexation. After hydroxylation of the two systems, the atomic ratios reached the nominal value of 2 for all R values. This accounted for the coprecipitation of the LDH phase from the HPIC micelle precursors. The study of the hydroxylated DHBC/M(II)-Al colloids at increasing complexation ratio emphasizes that different behaviors were induced by the nature of the divalent cation. The almost three times higher amount of DHBC polymer necessary to

avoid flocculation in the DHBC/Cu-Al compared to the DHBC/Mg-Al system was consistent with the lower Dh value and lower mean LDH particle size obtained for the former colloids. Considering a spherical shape of the colloids, a three times higher total surface area of the particles led to estimate that the mean size of the Cu-Al LDH particles was ca.1.7 times smaller than that of the Mg-Al ones.

It can be pointed out that the characterizations of the hydroxylated DHBC/M(II)-Al colloids which revealed (1) the presence of the (00l) reflections of the LDH phase in the XRD patterns, (2) the characteristic morphology of the muddled and anisotropic LDH particles observed by TEM, and (3) the M(II)/Al ratios of 2 determined by ICP – MS concur to clearly establish that coprecipitation of the M(II)-Al LDH phases occurs in the micellar core of the colloids.

3. 3. Progressive hydroxylation of DHBC/Cu-Al solutions at fixed complexation ratio (R = 0.8) and comparison with the Mg-Al system

To get more insights into the mechanisms of formation of the LDH phase in the core of the PAm_{10000}-*b*-PAA_{1500}/Cu(or Mg)-Al HPIC micelles along the hydroxylation step, the titration curves of the metal cation mixtures (Cu(or Mg)/Al = 2) using NaOH as the base in the presence of the DHBC (R = 0.8) were established (Figure 4). The metal cation contents in the hydroxylated colloids were determined by ICP-MS. The complexation ratio (R = 0.8) was chosen well above the flocculation thresholds in order to ensure the presence of stable colloids (Figure 3). Moreover, the titration curves and the cation contents in the macroscopic precipitates obtained at increasing pH in the absence of DHBC (R = 0) were also studied as references (Figure 4).

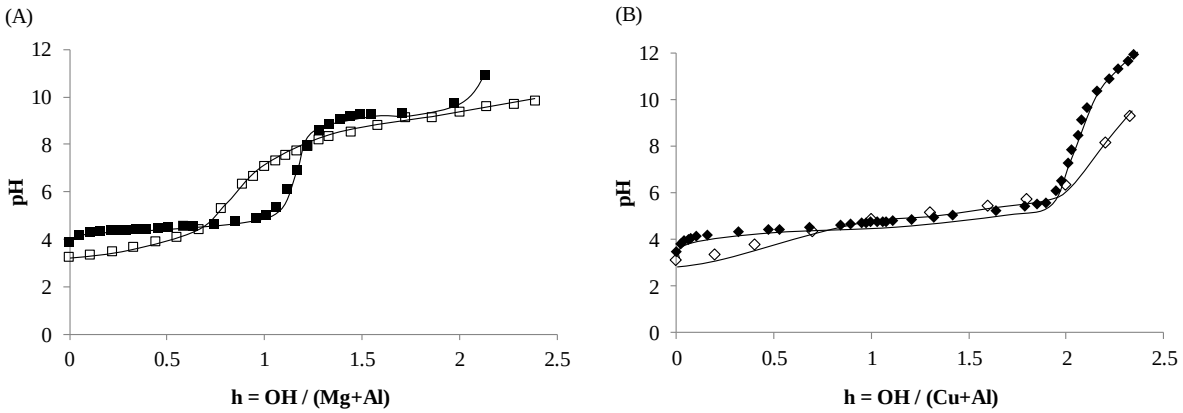

Figure 4: Titration curves of (A) the PAm_{10000}-*b*-PAA_{1500}/Mg-Al mixture at R = 0 (■) and R = 0.8 (□); (B) of the PAm_{10000}-*b*-PAA_{1500}/Cu-Al mixture at R = 0 (♦) and R = 0.8 (◊).

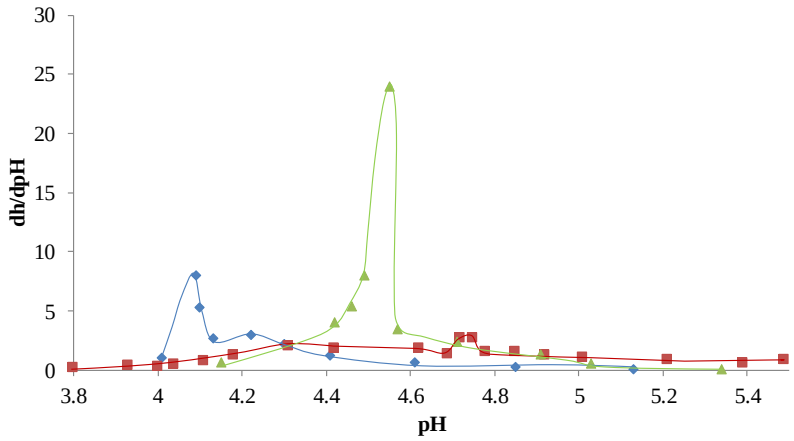

Figure 5: Derived dh/dpH curve as a function of pH of Cu (●), Al (▲) and Cu-Al mixture (■) at R = 0 (without DHBC).

3. 3. 1. Titration experiments in the absence of DHBC

In the case of the Mg-Al mixture, the titration curve without DHBC (R = 0) showed two plateaus (Figure 4A). The first one corresponded to precipitation of $Al(OH)_3$ with an end point h_{eq1} = 1.17 instead of the expected value h_{eq1} = 1 based on the stoichiometry of the solution. This shift was due to the carbonation of the cation solution of low concentration ($[Mg^{2+} + Al^{3+}]$ = 7.5 . 10^{-3} mol/L)) by dissolved CO_2. The second plateau corresponded to formation of Mg-Al LDH

with an end point h_{eq2} = 2.33 according to the total positive charge provided by the metal cations. In the case of the Cu-Al mixture at R = 0, only one plateau at pH ~ 4.4 followed by an increase to the end point h_{eq} = 2.33 at pH = 8.5 corresponding to total precipitation was observed during the titration, as previously reported (Figure 4B). In order to get more insights into the hydroxylation process, the derived curves dh/dpH as a function of pH of the Cu^{2+}-Al^{3+} mixture and of Cu^{2+} and Al^{3+} ions alone were depicted on Figure 5. They allowed putting clearly into evidence the pH values of precipitation of the different phases. In the case of the Cu^{2+} derived curve, a peak was observed at pH = 4.1, followed by a broader peak with a maximum at pH = 4.2 accounting for precipitation of hydroxylated carbonate copper species. In the case of the derived curve of Al^{3+}, a maximum was observed at pH = 4.5 which corresponded to precipitation of $Al_{13}O_4(OH)_{24}(H_2O)_{12}^{7+}$ (Al_{13} Keggin polycation) species in the speciation diagram (Baes, 1976). It is then noteworthy that the single Cu-containing species precipitated 0.4 pH unit below the single Al-containing ones. Such behavior could have induced a direct coprecipitation of the Cu-Al LDH phase during titration of the Cu^{2+} and Al^{3+} ions mixture by the alkaline solution as suggested by Boclair and Braterman (1998). However, this is inconsistent with the derived curve dh/dpH as a function of pH of the $Cu^{2+}$and Al^{3+} mixture exhibiting two maxima at pH = 4.3 and 4.75. They revealed two steps of precipitation and thus, a sequential mechanism of formation of Cu-Al LDH.

3. 3. 2. Titration experiments in the presence of DHBC

Addition of PAm_{10000}-*b*-PAA_{1500} DHBC to both Cu-Al and Mg-Al metal cation mixture solutions led to a decrease of the initial pH from 3.9 to 3.3 (pH = 3.3 before the hydroxylation step). This was due to complexation reaction of the metal ions by the carboxylic acid functions of the PAA blocks leading to proton release in solution and formation of the acrylate - M^{n+} complex. In comparison to the titration curves obtained in the absence of DHBC, that of the Mg-Al system obtained in the presence of PAm_{10000}-*b*-PAA_{1500} DHBC (R = 0.8) presented less

distinct plateaus exhibiting a slight slope, and less abrupt pH increase at their end (Figure 4A). Noteworthy, h_{eq1} corresponding to the complete precipitation of $Al(OH)_3$ was shifted from 1.17 in DHBC-free conditions to 0.67 in the presence of DHBC (R = 0.8), with concurrently a pH increase extended on a larger h range from 0.7 to 1.5. The shift of the h_{eq1} to a lower value accounted for the complexation of part of the Al^{3+} ions yielding a reduced amount of Al^{3+} ions available for the hydroxylation reaction and the formation of $Al(OH)_3$. These changes in the general shape of the curve in comparison to DHBC-free conditions accounted for different speciation of metal cations in solution. It contains free cationic species together with acrylate complexed metal cations with varying complexing ratios. Therefore, hydroxylation reaction occurs on a wide range of hydroxylation ratios and pHs. For the Cu-Al cation mixture in the presence of DHBC, changes in the general shape of the titration curve were by far less pronounced (Figure 4B). This could be expected since the two very close precipitation steps, only separated by 0.45 pH unit in the absence of DHBC, will be smoothed in the presence of DHBC.

In summary, comparison of the titration curves of Cu^{2+}- Al^{3+} and Mg^{2+}- Al^{3+} ionic solutions (Figures 4A and B) showed that the general mechanism of LDH formation was similar in the absence or in the presence of PAm_{10000}-*b*-PAA_{1500} DHBC and, importantly, was sequential in the two systems. The Mg-Al LDH coprecipitation was delayed on a larger range of hydroxylation ratio in the presence of DHBC due to the competition between metal hydroxylation and complexation reaction by PAA blocks (which led to the formation of exclusively DHBC/Al^{3+} HPIC micelles). The complexation reaction influenced the behavior of the DHBC/Cu^{2+}-Al^{3+} mixture in a smaller extent because the two precipitation steps of the LDH phase appeared almost merged.

3. 3. 3. Speciation of the precipitates obtained in the absence of DHBC

The Cu and Al yields were measured in the macroscopic precipitates formed all along the process of titration of the Cu-Al mixture using NaOH at R = 0. Noteworthy, Cu and Al precipitated abruptly and in a parallel way since the beginning of the hydroxylation (Figure 6C). The Cu and Al yields at the pH values corresponding to the two maxima observed in the derived curve (dh/dpH = f(pH), Figure 5)) were particularly examined. At pH = 4.1, Cu was not present in the precipitate and the Al yield reached ca. 28%. The Al yield abruptly increased to 60% at pH = 4.3 while that of Cu increased in a lower extent to ca. 10%. The Cu and Al yields then reached 56.5% and 100%, respectively, at pH = 4.75 corresponding to the second maximum in the derived dh/dpH = f(pH) curve, and reached 84.8% and 100%, respectively, at pH = 5.1 corresponding to the end of this second peak. These results allowed to assign the first maximum in the derived curve (pH = 4.3) to aluminum poly(hydr)oxide species because practically only aluminum was precipitated. The Cu and Al yields obtained at the second maximum at pH = 4.8 would correspond to the establishment of di-hydroxo bridges between copper and aluminum poly(hydr)oxide species thus forming the precursors of the Cu-Al LDH phase which precipitated at pH = 5.1. Between pH 4.8 and 9 the Al yield decreased slightly from 100% to 95% when concurrently the Cu yield increased from 85% to 98%. As complete coprecipitation of the Cu-Al LDH phase has occurred, the slightly higher final Cu yield could be the result of formation of excess Cu-containing phase, which could not be identified by XRD because in too low amount.

Therefore, from careful examination of the titration curves and of the Cu and Al yields in the precipitates during the titration experiments of the Cu-Al mixture in the absence of DHBC (R = 0) (Figure 6C), a mechanism of formation of the LDH phase in two steps can be suggested. The first step occurring at pH = 4.3 corresponded to precipitation of aluminum oxohydroxide framework, containing mainly Al_{13} species. Their polycondensation was then going on between

pH = 4.3 and 4.75 with, at the same time, incorporation of copper leading to complete precipitation of the Cu-Al LDH phase.

Regarding the Mg-Al system, the evolution of the Mg and Al yields in the macroscopic precipitates obtained at R = 0 upon hydroxylation (Figure 6A) were consistent with the mechanism of formation of Mg-Al LDH already described (Boclair and Braterman, 1999; Rhada and Kamath, 2003; Seron and Delorme, 2008). Al^{3+} and Mg^{2+} were present as free cations in solution at pH = 4.5. The Al yield increased abruptly above pH = 4.5 reaching 76% at pH = 5 due to the formation of aluminum poly(hydr)oxide precipitate precursors of $Al(OH)_3$. Concurrently the Mg yield increased in a moderate rate to 14%. The Al yield reached 94% at pH = 8 corresponding to complete precipitation of $Al(OH)_3$ while that of Mg increased only slightly to 18%. Then the Al yield decreased from 94 to 78% between pH 8 and 9 when, remarkably at the same time, the Mg yield increased abruptly from 18 to 40%. This was in agreement with the mechanism generally accepted of partial dissolution of $Al(OH)_3$ into $Al(OH)_4^-$ species above pH 8 followed by coprecipitation of dissolved aluminum and free magnesium ions to give dihydroxo $Mg(OH)_2Al$ bonds initiating the formation of the Mg-Al LDH phase (Boclair and Braterman, 1999; Seron and Delorme, 2008)). These dihydroxo $Mg(OH)_2Al$ bonds and the formation of the LDH phase occurred in a larger extent when the pH was raised to 9.6 because the Mg yield reached 85% in the colloids.

By comparing the behavior of the Cu-Al and Mg-Al systems upon progressive hydroxylation in the absence of DHBC, it can be underlined that the Cu-Al LDH was totally formed at pH ~ 5.5 from aluminum poly(hydr)oxide precursor species while Mg-Al LDH was formed at pH ~ 8 from $Al(OH)_3$ precursor. Beside the different nature of the Al-containing species in the LDH precursors, the different behavior of the Mg and Cu-based systems also accounted for the lower solubility of $Cu(OH)_2$ (pKs = 18.7) compared to $Mg(OH)_2$ (pKs = 10.8). That makes very close

the precipitation pHs of $Cu(OH)_2$ and Cu-Al LDH, while they were well separated in the case of $Mg(OH)_2$ and Mg-Al LDH.

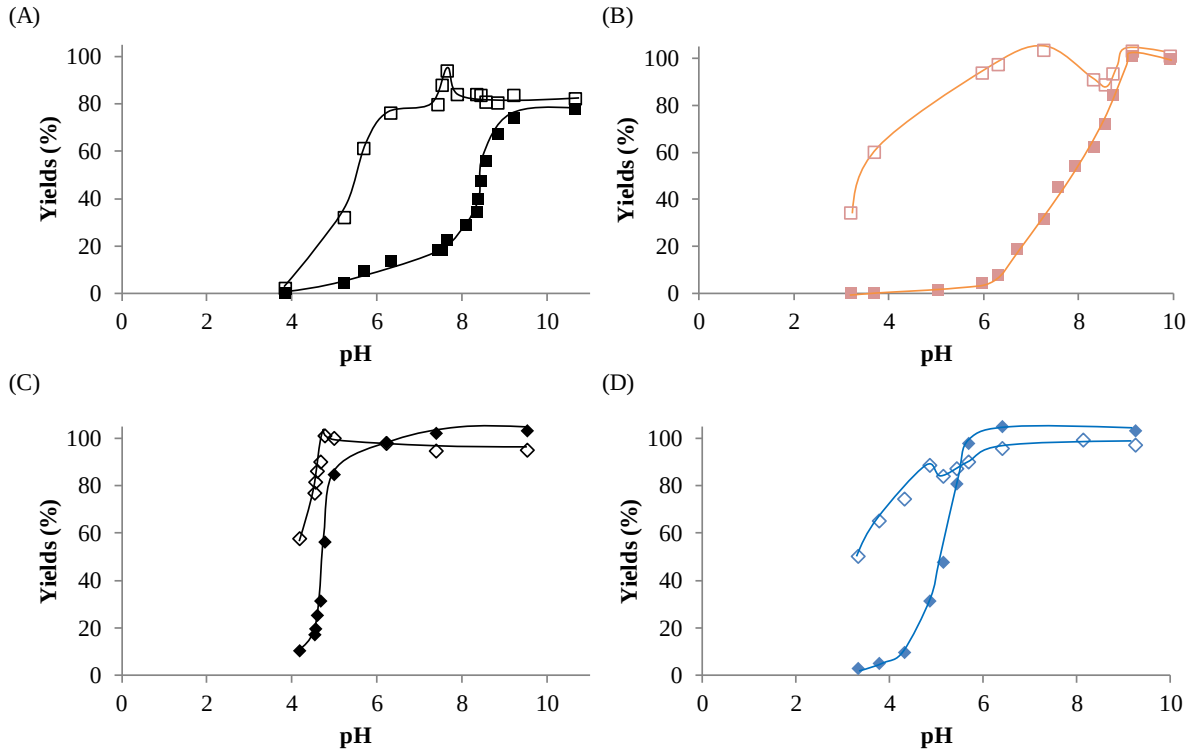

Figure 6: Cationic yields of (A) Mg^{2+} (■), Al^{3+} (□) in the macroscopic precipitates at R = 0; (B) Mg^{2+} (■), Al^{3+} (□) in the PAm_{10000}-*b*-PAA_{1500}/Mg-Al colloids at R = 0.8, (C) Cu^{2+} (♦), Al^{3+} (◊) in the macroscopic precipitates at R = 0; (D) Cu^{2+} (♦), Al^{3+} (◊) in the PAm_{10000}-*b*-PAA_{1500}/Cu-Al colloids at R = 0.8 as a function of pH value determined by ICP-MS.

3. 3. 4. Speciation of the colloids obtained in the presence of DHBC

In the presence of DHBC, the evolutions of the metal cation yields as a function of pH were reported on Figure 6D for the PAm_{10000}-*b*-PAA_{1500}/Cu-Al and on Figure 6B for the PAm_{10000}-

b-PAA_{1500}/Mg-Al colloids (R = 0.8). In the two cases, about 35 to 60% of Al cations were initially complexed at pH = 3.3. At pH = 4.3 the Cu and Al yields reached 9.8% and 74.5%, respectively, and were thus in the same range, as in the absence of DHBC. At pH = 4.75 the Cu and Al yields increased to 31.5% and 88.5%, respectively, being lower than in the absence of DHBC (84.8% and 100%, respectively) suggesting that, in the presence of DHBC, the precipitation of the LDH phase was slightly shifted toward higher pH value. Indeed, complete precipitation with Cu and Al yields reaching 94% and 98%, respectively, occurred at pH = 6 in the absence of DHBC. Complete precipitation occurred at pH = 6.4, thus about 0.4 pH unit above, in the presence of DHBC, with Cu and Al yields reaching 98% and 100%, respectively. The evolution of Cu^{2+} and Mg^{2+} atomic fractions ($M^{2+}/(M^{2+} + Al^{3+})$) in the precipitated colloids as a function of pH during hydroxylation of the DHBC/M(II)-Al mixtures were reported on Figure 7. It clearly showed that precipitation occurred in a very different pH range from 4 to 6 for Cu-Al mixture and from 6 to 9 for Mg-Al mixture. It is associated with a higher slope of the curve in the former case (0.40 for Cu-Al versus 0.22 for Mg-Al), which probably indicated a higher rate of formation of the Cu-Al di-hydroxo bridges compared to the Mg-Al hydroxo ones. Noteworthy, the maximum atomic fraction of divalent cation of ca. 0.64 was close to the nominal value 0.66 in both cases.

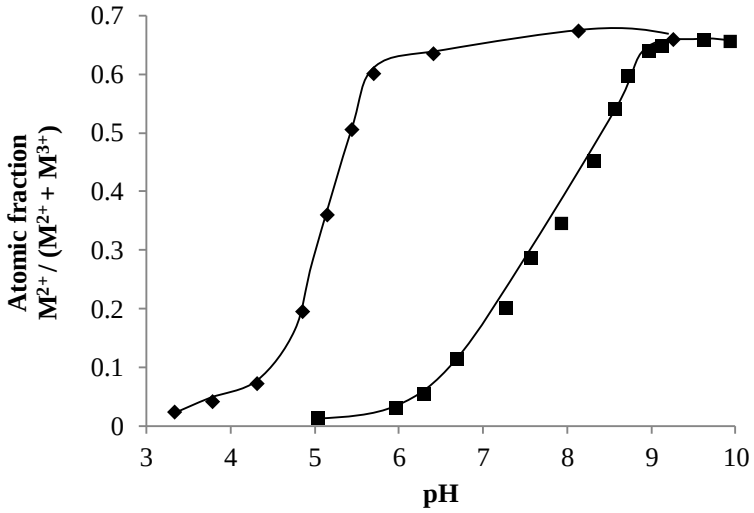

Figure 7: Evolution of the Cu^{2+} (♦) and Mg^{2+} (■) atomic fractions as a function of pH during hydroxylation of the (Cu^{2+} + Al^{3+}) and (Mg^{2+} + Al^{3+}) mixtures by NaOH in presence of PAm_{10000}-*b*-PAA_{1500} at R = 0.8.

XRD and TEM analyses revealed that the mean size and aggregation degree of the Cu-Al LDH colloids are lower than those of the Mg-Al LDH ones. It must be noticed that hydroxylation was achieved at pH = 8.5 in the DHBC/Cu-Al system and at pH = 10 in the DHBC/Mg-Al system, therefore about 2 - 3 and 1.5 pH units, respectively, above the complete precipitation of the Cu-Al and Mg-Al LDH phases, as observed on Figure 7. Cu-Al LDH was thus precipitated at a slightly higher supersaturation ratio than the Mg-Al LDH. This feature and the faster precipitation of the LDH could account for a higher nucleation rate and then a lower mean particle size and aggregation degree of the Cu-Al LDH particles.

3. 4. Insights about the mechanisms of formation

The mechanism of formation of Cu-Al LDH was scarcely described in previous works. It was a typical case where the relatively low solubility of $Cu(OH)_2$ and the high solubility of $Al(OH)_3$ led to consider as possible the direct one-step formation of Cu-Al LDH. Boclair and Braterman

(1998) indeed claimed the direct formation of sulfated Cu-Al LDH (Cu/Al = 2), corresponding to the natural mineral called woodwardite, but did not give experimental pieces of evidence. In the present work, we showed that a simple copper-containing hydroxide precipitated about 0.4 pH unit below the aluminum hydroxide ones and both at pH ≤ 5. However, the derived curve dh/dpH as a function of pH of the Cu-Al metal cations mixture titrated with an alkaline solution revealed two clear maxima according to a precipitation mechanism in two steps of the LDH. The key feature is that the first step at pH = 4.3 with concurrently the presence of almost only aluminum species in the precipitate, evidenced that aluminum poly(hydr)oxide species formed at this pH were the true precursors of the LDH phase. The LDH was formed in the second precipitation step at pH= 4.8 by combination of the aluminum poly(hydr)oxide species with dissolved copper-based species. This showed that the involvement of copper in Cu-Al LDH phase was more thermodynamically favorable than in $Cu(OH)_2$. These results demonstrated that direct coprecipitation in one-step of LDH probably never occurred when aluminum was the trivalent cation. Moreover, the nature of the aluminum precursor of the Cu-Al LDH was in agreement with the speciation of aluminum hydroxide species existing in the pH range 4 – 5 of coprecipitation of the LDH. In the case of Mg-Al mixture the results obtained in the present work were in line with those depicted in our previous study (Layrac et al., 2014). A sequential mechanism in two steps of formation of LDH was evidenced with first precipitation of $Al(OH)_3$, then dissolved and combined with Mg^{2+} ions in solution to form the Mg-Al LDH phase at a pH about 2 units below that of precipitation of $Mg(OH)_2$.

In the presence of DHBC, the general mechanism of formation of the LDH was similar in both Cu-Al and Mg-Al systems to those in the absence of DHBC. However, the coprecipitation of the LDH was slightly shifted at higher pH due to competition between hydroxylation and complexation of the ionic species by the PAA block of DHBC. Moreover, differences were observed for the micelles formed in the two types of DHBC/M^{2+}-Al^{3+} systems. In the case of

DHBC/Mg^{2+}-Al^{3+}, intermediate DHBC/Al^{3+} HPIC micelles were exclusively formed. The DHBC/Al^{3+} HPIC micelles led to DHBC/Mg-Al LDH colloids upon hydroxylation until pH = 10 following the mechanism previously described with first dissolution of $Al(OH)_3$ formed at ~ pH = 6 and second, progressive integration of Mg^{2+} in the micellar core acting as a nanoreactor. In this two-step process, increase of Mg^{2+} and Al^{3+} yields in the precipitated colloids as the pH increased was obviously non-concomitant starting two units higher for Mg^{2+}, i. e. after complete hydroxylation of Al^{3+} ions. In the case of DHBC/Cu^{2+}-Al^{3+}, higher Cu^{2+}/Al^{3+} atomic ratios were observed all along hydroxylation, whatever the complexation ratio, and the flocculation threshold R1 value was about three times higher than in DHBC/Mg^{2+}-Al^{3+} (0.43 for Cu-Al and 0.13 for Mg-Al). DHBC/Cu^{2+}-Al^{3+} micelles then contained Al^{3+} in large amount and Cu^{2+} in minor amount. This was in agreement with the remarkable affinity of the PAA block of the polymer for Cu^{2+} by far higher than for Mg^{2+}. The reasons why the Cu-Al LDH particles are smaller than the Mg-Al LDH ones are: i) the higher precipitation rate of the Cu-Al LDH in the micellar core upon hydroxylation occurring in a pH range of ~ 2 pH units, instead of more than ~ 3 pH units for Mg-Al LDH, and ii) the high supersaturation ratio of coprecipitation. This was in agreement with the three times higher amount of DHBC necessary to stabilize the Cu-Al LDH particles than the Mg-Al LDH ones at the flocculation threshold (R1).

All these results led us to suggest a mechanism of formation of Cu-Al LDH reported in scheme 1.

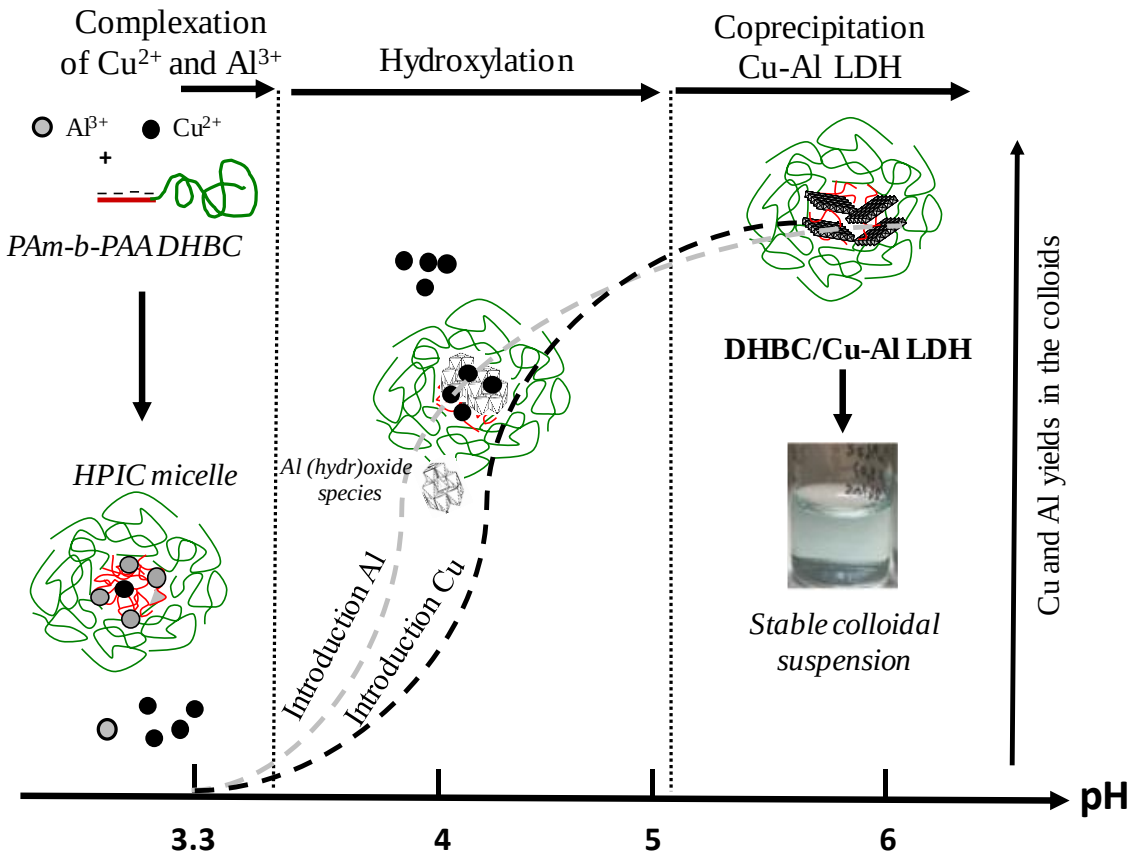

Scheme 1: Schematic representation of the formation of the DHBC/Cu-Al LDH colloids in water by progressive hydroxylation.

4. Conclusions

The formation of Cu-Al LDH phase represented a case study among this family of layered materials because firstly, coprecipitation occurs at a quite low pH due to the close solubilities of the simple $Al(OH)_3$ and $Cu(OH)_2$ hydroxides, and secondly, introduction of Cu^{2+} in the octahedral sheets is not obvious due to the Jahn-Teller effect. The mechanism of LDH formation was not yet clearly established and direct coprecipitation by co-hydroxylation of the two cations was suggested in the literature. This was a strong incitement to compare the coprecipitation of the Cu-Al LDH phase by conventional progressive hydroxylation of a mixture of Cu^{2+} and Al^{3+} ions (Cu^{2+}/Al^{3+} = 2) and of this mixture of cations in the presence of

PAm-*b*-PAA DHBC polymer. Complexation of Cu^{2+} and Al^{3+} ions by PAA blocks must indeed lead to HPIC micelles and then to coprecipitation of the Cu-Al LDH in a confined nanoreactor able to influence the mechanism of formation and the properties of the Cu-Al LDH particles. A specific feature was that the high affinity of acrylate functions of the DHBC polymer for Cu^{2+} made poorly competitive the complexation of Cu^{2+} and Al^{3+} by PAA. Careful analysis of the titration curve of the Cu^{2+}-Al^{3+} ion mixture by NaOH and of the composition of the macroscopic precipitates in the absence of DHBC, clearly established a sequential mechanism of formation of Cu-Al LDH at pH $\leq$ 5. It goes through the presence first of aluminum poly(hydr)oxide precursors which then incorporate the copper cations. The same mechanism prevails in the presence of PAm-*b*-PAA DHBC polymer and stable aqueous colloids of Cu-Al LDH have been obtained. The HPIC micelles initially formed at lower complexation degree contain almost exclusively aluminum. Then Cu^{2+} content increases as the complexation degree increases. Upon hydroxylation, the Al^{3+} and Cu^{2+} contents in the colloids increase concurrently in a narrow pH range of about 2 units and led to pure Cu-Al LDH phase at ~ pH = 5.5. The metal complexation degree allowed controlling the particle stability and the Cu-Al LDH particle sizes. Smaller average particle sizes of the Cu-Al LDH particles were obtained compared to the Mg-Al LDH particles, which could result from the rapid nucleation and complete coprecipitation of the LDH phase. These low particle sizes were consistent with the higher DHBC amount needed in the DHBC/Cu-Al mixture to stabilize the colloidal particles at the flocculation threshold R1. Poorly aggregated Cu-Al LDH particles were evidenced by TEM, and their average size varied in the range from 30 to 40 nm.

These results showed that the sequential mechanism of LDH formation is probably involved in all aluminum-containing LDH, though with a different nature of the precursors in solution depending on the nature of the divalent cation. Using DHBC in aqueous solution to obtain stable colloidal suspensions of LDH can potentially be extended to a wide variety of couples of

divalent and trivalent cations because Mg^{2+} and Cu^{2+} represent two extreme cases regarding solubility of the hydroxides and affinity for complexation by DHBC.

References

Baes, R. E. M. C. F., 1976. The hydrolysis of cations. J. Wiley, New-York.

Boclair, J. W., Braterman, P. S., 1998. One-step formation and characterization of Zn(II)-Cr(III) layered double hydroxides $Zn_2Cr(OH)_6X$ (X = Cl, ½ SO_4). Chem. Mater. 10, 2050 – 2052.

Boclair, J. W., Braterman, P. S., 1999. Layered double hydroxide stability. 1. Relative stabilities of layered double hydroxides and their simple counterparts. Chem. Mater. 11, 298 - 302.

Boclair, J. W., Braterman, P. S., Jiang, J., Lou, S., Yarberry, F., 1999. Layered double hydroxide stability. 2. Formation of Cr(III)-containing layered double hydroxides directly from solution. Chem. Mater. 11, 303-307.

Bouyer, F., Gérardin, C., F. Fajula, F., Putaux, J. L., Chopin, T. 2003. Role of double-hydrophilic block copolymers in the synthesis of lanthanum-based nanoparticles. Colloids and Surfaces A: Physicochemical and Engineering Aspects. 217, (1–3), 179-184.

Bouyer, F., Sanson, N., Destarac M., Gérardin, C., 2006. Hydrophilic block copolymer-directed growth of lanthanum hydroxide nanoparticles. N. J. C., 30, 399 – 408.

Bukhtiyarova, M. V., 2019. A review on effect of synthesis conditions on the formation of layered double hydroxides. J. Solid State Chem. 269, 494 – 506.

Cavani, F., Trifiro, F., Vaccari, A., 1991. Hydrotalcite-type anionic clays: preparation, properties and applications. Catal. Today. 11, 173 – 301.

Depège, C., Bigey, L., Forano, C., De Roy, A., Besse, J. P., 1996. Synthesis and characterization of new copper-chromium layered double hydroxides pillared with polyoxovanadates. J. Solid State Chem. 126, 314 – 323.

Gérardin, C., Sanson, N., Bouyer, F., Fajula, F., Putaux, J. L., Joanicot, M., Chopin,T., 2003. Highly Stable Metal Hydrous Oxide Colloids by Inorganic Polycondensation in Suspension. Angew. Chem. Int. Ed. 42, 3681 – 3685.

Irving, H., Williams, R. J. P., 1953. The stability of transition metal complexes. J. Chem. Soc. 3192 – 3210.

Layrac, G., Destarac, M., Gérardin, C., Tichit, D., 2014. Highly stable layered double hydroxide colloids: A direct aqueous synthesis route from hybrid polyion complex micelles. Langmuir. 30, 9663 − 9671.

Layrac, G., Gérardin, C., Tichit, D., Harrisson, S., Destarac, M., 2015. Hybrid polyion complex micelles from poly(vinylphosphonic acid) based double hydrophilic block copolymers and divalent transition metal ions. Polymer. 72, 292 – 300.

Li, D., Cai, Y., Ding, Y., Li, R., Lu, M., Jiang, L., 2015. Layered double hydroxides as precursors of Cu catalysts for hydrogen production by water-gas shift reaction. Int. J. Hydrogen Energ. 40, 10016 – 10025.

Li, D., Xu, X., Xu, J., Hou, W., 2011. Poly(ethylene glycol) haired layered double hydroxides as biocompatible nanovehicles: Morphology and dispersity study. Colloids and Surfaces A: Physicochem. Eng. Aspects. 384, 585– 591.

Lu, H., Sui, M., Yuan, B., Wang, J., Lv, Y., 2019. Efficient degradation of nitrobenzene by Cu-Co-Fe-LDH catalyzed peroxymonosulfate to produce hydroxyl radicals. Chem. Eng. J. 357, 140 – 149.

Lucarelli, C., Molinari, C., Faure, R., Fornasari, G., Gary, D., Schiaroli, N., Vaccari, A., 2018. Novel Cu-Zn-Al catalysts obtained from hydrotalcite-type precursors for middle-temperature water-gas shift applications. Appl. Clay Sc. 155, 103 – 110.

Mao, N., Zhou, C. H., Tong, D. S., Yu, W. H., Lin, C. X. C., 2017. Exfoliation of Layered double hydroxide solids into functional nanosheets. Appl. Clay Sc., 144, 60 – 78.

Marchi, A. J., Gordo, D. A., Trasarti, A. F., Carlos R. Apesteguıa, C. R., 2003. Liquid phase hydrogenation of cinnamaldehyde on Cu-based catalysts, Appl. Catal. A: General. 249, 53 – 67.

Sanson, N., Bouyer, F., Destarac, M., In, M., Gérardin, C., 2012. Hybrid Polyion Complex Micelles Formed from Double Hydrophilic Block Copolymers and Multivalent Metal Ions: size control and nanostructure. Langmuir, 28, 3773-3782.

Park, I. Y., Kuroda, K., Kato, C., 1990. Preparation of complex copper aluminum double hydroxide phases from copper(II) ammine complex solutions. Solid State Ionics. 42, 197 – 203.

Raciulete, M., Layrac, G., Tichit, D., Marcu, I. M., 2014. Comparison of Cu_xZnAlO mixed oxide catalysts derived from multicationic and hybrid LDH precursors for methane total oxidation. Appl. Clay Sc. 477, 195 - 204.

Radha, A. V., Kamath P. V., 2003. Aging of trivalent metal hydroxide/oxide gels in divalent metal salt solutions: Mechanism of formation of layered double hydroxides (LDH). Bull. Mater. Sci. 26, 661 – 666.

Rajamathi, M., Kamath, P. V., 2000. Ageing behaviour of unary hydroxides in trivalent metal salt solutions: Formation of layered double hydroxide (LDH)-like phases. Bull. Miner. Sci. 23, 355 – 359.

Said, S., Elhossieny, M., Riada, M., Mikhail, S., 2018. Pristine Cu (Co)/Fe layered double hydroxides (Co(Cu)/Fe-LDH) as active catalysts for the transalkylation of toluene to trimethylbenzenes. Molecular Catal. 445, 213 – 222.

Sanson, N., Putaux, J. L., Destarac, M., Gérardin, C., Fajula, F., 2005. Hybrid organic-inorganic colloids with a core-corona structure : A transmission electron microscopy investigation. Macromol. Symp. 226, (1), 279-288.

Seron, A., Delorme, F., 2008. Synthesis of layered double hydroxides (LDH) with varying pH: A valuable contribution to the study of Mg/Al LDH formation mechanism. J. Phys. Chem. Solids. 69, 1088 – 1090.

Tarasov, K., Houssein, D., Destarac, M., Marcotte, M., Gérardin, C., Tichit, D. 2013. Stable aqueous colloids of ZnS quantum dots prepared using double hydrophilic block copolymers. New J. Chem. 37, 508 – 514.

Trujillano, R., Holgado, M. J., González, J. L., Rives, V., 2005. Cu–Al–Fe layered double hydroxides with CO_3^{2-} and anionic surfactants with different alkyl chains in the interlayer. Solid State Sc. 7, 931 – 935.

Wang, N. Liu, S., Zhang, J., Wu, Z., Chen J., Sun, D., 2005. Lamellar phase in colloidal suspensions of positively charged LDHs platelets. Soft Matter. 1, 428 - 430.

Wang, Q., O'Hare, D., 2012. Recent advances in the synthesis and application of layered double hydroxide (LDH) nanosheets. Chem. Rev. 112, 4124−4155

Xu, Z. P., Stevenson, G. S., Lu, C. Q., Lu, G. Q., Bartlett, P. F. Gray, P. P., 2006. Stable suspension of layered double hydroxide nanoparticles in aqueous solution. J. Am. Chem. Soc. 128, 36 – 37.

Zhang, Y., Li, C., Yu, C., Tran, T., Guo, F., Yang, Y., Yu, J., Xu, G., 2017. Synthesis, characterization and activity evaluation of Cu-based catalysts derived from layered double hydroxides (LDHs) for DeNOx reaction. Chem Eng. J. 330, 1082 – 1090.

Zhang, Y., Li, H., Du, N., Zhang, R., Hou, W., 2016. Large-scale aqueous synthesis of layered double hydroxide single-layer nanosheets. Colloids Surf. A: Physicochem Eng. Aspects, 501, 49 – 54.

Supplementary information

Synthesis of Cu-Al layered double hydroxide: Mechanism of formation and preparation of stable colloids

G. Layrac[1,†], M. Destarac[2], S. Harrisson[2], D. Tichit[1*], C. Gérardin[1*]

[1]ICGM, Univ. Montpellier, CNRS UMR 5253, ENSCM, Montpellier, France

[3]IMRCP, UMR 5623 CNRS-UPS Toulouse, France

Corresponding authors.

E-mail address: didier.tichit@enscm.fr; corine.gerardin@enscm.fr

[†]Present address: ICPEES, CNRS UMR 7515, ECPM-Université de Strasbourg, France

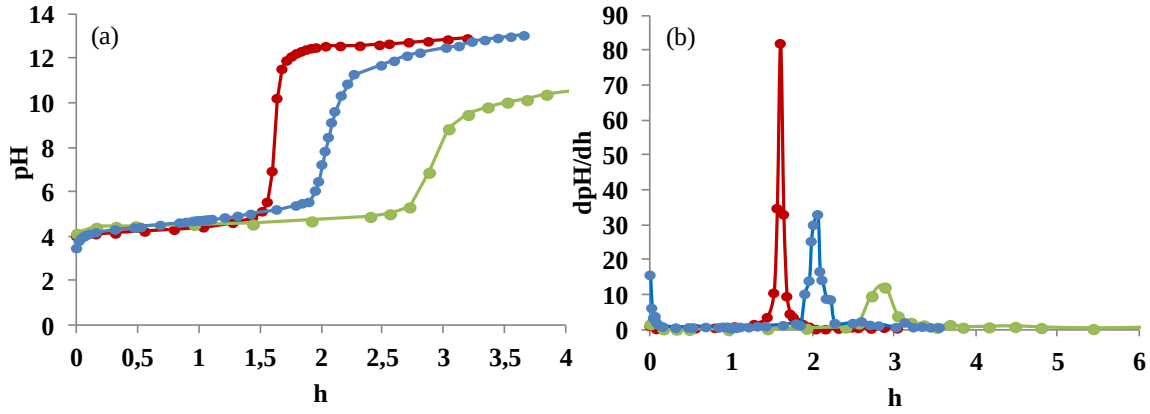

Figure S1: Evolution of the pH (a) and of dpH/dh (b) in function of h at R = 0 (without DHBC) during titration of Cu^{2+} (0.10 $mol.l^{-1}$) (●), Al^{3+} (0.05 $mol.l^{-1}$) (●) and (Cu^{2+} + Al^{3+}) (0.15 $mol.l^{-1}$) (●) by NaOH (0.2 $mol.l^{-1}$)).

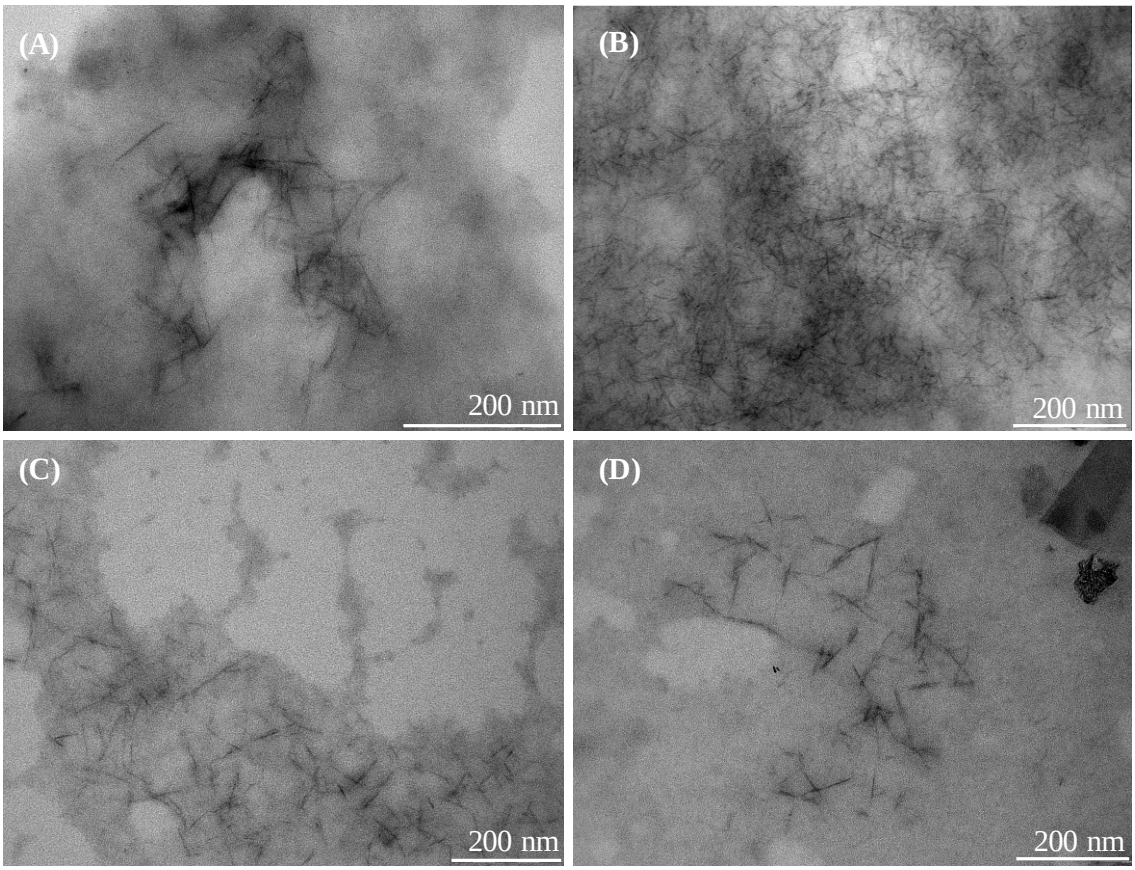

Figure S2: TEM images of (A) Cu-Al macroscopic precipitate (R = 0), and of the DHBC/Cu-Al LDH colloids at (B) R = 0.33, (C) R = 0.53 and (D) = 0.66.

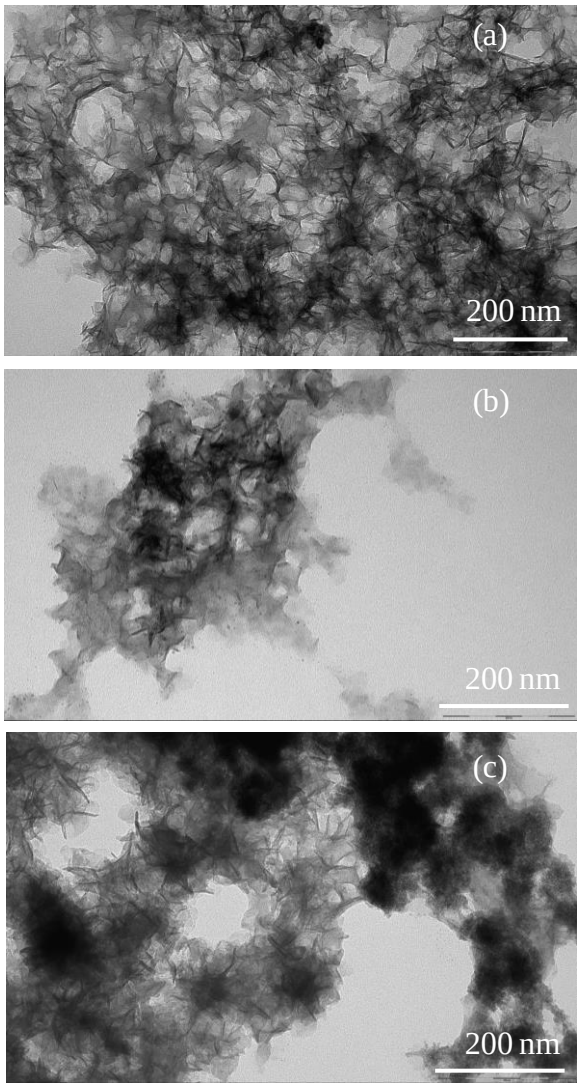

Figure S3: TEM images of (A) Mg-Al macroscopic precipitate (R = 0.05), and DHBC/Mg-Al LDH colloids at (B) R = 0.20 and (C) R = 0.33.